Velocity probability distribution scaling in wall-bounded flows at high Reynolds numbers

M.-W. Ge,[1] Xiang I. A. Yang,[2,*] and Ivan Marusic[3]
[1]*School of Renewable Energy, North China Electric Power University, Beijing, China*
[2]*Mechanical and Nuclear Engineering, Penn State University, State College, Pennsylvania 16802, USA*
[3]*Department of Mechanical Engineering, University of Melbourne, Parkville, Victoria 3010, Australia*

(Received 29 August 2018; published 7 March 2019)

Probability density functions (PDFs) give well-rounded statistical descriptions of stochastic quantities and therefore are fundamental to turbulence. Wall-bounded turbulent flows are of particular interest given their prevalence in a vast array of applications, but for these flows the scaling of velocity probability distribution is still far from being well founded. By exploiting the self-similarity in wall-bounded turbulent flows and modeling velocity fluctuations as results of self-repeating processes, we present a theoretical argument, supported by empirical evidence, for a universal velocity PDF scaling in high-Reynolds-number wall turbulence.

DOI: 10.1103/PhysRevFluids.4.034101

I. INTRODUCTION

Wall-bounded turbulent flows [1] are prevalent in a vast array of applications, from environmental flows, such as their role in gas exchange at the air-sea interface through the atmospheric surface layer, to engineering, where these flows account for over 50% of the drag through skin friction on aircraft and over 95% of the energy losses in long pipe transport networks. As quantities including velocity and pressure in a wall-bounded turbulent flow are generally stochastic (although the Navier-Stokes equation is deterministic), probability distributions are a useful tool for describing turbulence. A notable example is the use of the probability density function (PDF) method in turbulence combustion where a set of transport equations for the velocity-composition PDFs is solved [2,3].

The study of velocity PDFs in wall-bounded flows dates back to the 1950s [4]. The focus was on the logarithmic layer within which the flow is self-similar. Dinavahi *et al.* [5] concluded that the streamwise velocity PDF, i.e., $P(u)$, is independent of both the Reynolds number and the wall-normal distance in the logarithmic region. The proposed self-similarity was later refined by Lindgren *et al.* [6], who postulated a different universal velocity PDF scaling, i.e., $P(u/u_{\rm rms})$, where $u_{\rm rms}$ is the root mean square of the streamwise velocity fluctuation. These early works are, by and large, focused on the streamwise velocity component. The arguments are usually heuristic and the postulated scalings are compared to data at only low and moderate Reynolds numbers, where the extent of the logarithmic range is limited [7]. Due to the developments in experimental measurement techniques and high performance computing, data at high and extreme Reynolds numbers have become available from both laboratory experiments [8–10] and high-fidelity direct numerical simulations (DNSs) [11–13]. Figure 1(a) shows the streamwise velocity PDFs in boundary layer flows at friction Reynolds numbers from $\mathrm{Re}_\tau \approx 2800$ to $\mathrm{Re}_\tau \approx 13\,000$ and Fig. 1(b)

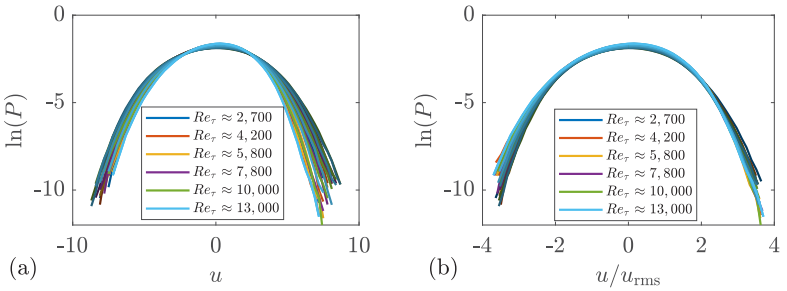

FIG. 1. (a) Streamwise velocity PDF in the logarithmic layer, i.e., $3\sqrt{\mathrm{Re}_\tau} < z^+, z/\delta < 0.2$, where Re_τ is the friction Reynolds number, z is the wall-normal coordinate, and δ is the boundary layer height. Details of this data set are presented later. Data at different Reynolds numbers are color coded. For data at a given Reynolds number, darker colors are used for velocities closer to the wall. (b) Same as (a) but plotted as a function of $u/u_{\rm rms}$, where $u_{\rm rms}$ is the root mean square of the streamwise velocity fluctuation.

shows the same PDFs but as a function of $u/u_{\rm rms}$. While a better data collapse is found for $P(u/u_{\rm rms})$, it is probably clear from Fig. 1 that neither $P(u)$ nor $P(u/u_{\rm rms})$ is universal. It is therefore timely to revisit the scaling of velocity PDFs in wall-bounded turbulent flows.

The rest of the paper is organized as follows. In Sec. II we use Townsend's attached-eddy model [14–16], the hierarchical random additive model [17–20], and the large-deviation theory to make predictions of the scaling of velocity PDFs in high-Reynolds-number wall-bounded flows. The discussion focuses on the scaling of the tails of velocity PDFs. Details of the data sets are presented in Sec. III. The predicted scalings are compared to experimental measurements and numerical simulation data in Sec. IV. Concluding remarks are given in Sec. V.

II. THEORY

Invoking Townsend's attached-eddy hypothesis [14,16–18] and using data up to $\mathrm{Re}_\tau \approx 13\,000$, in this work we will show that the tails of the velocity PDF in wall-bounded flows follow the scaling $\exp[-N_z f_i(u_i/N_z)]$ in the logarithmic range at both moderate and high Reynolds numbers, where the scaling factor $N_z \sim \ln(\delta/z) \sim \langle u_i^2 \rangle \sim \ln\{\langle \exp[q_0 u_i(z)] \rangle\}$ $(i = 1, 2)$, u_1 and u_2 are velocity fluctuations in the streamwise and the spanwise directions, respectively, f_i $(i = 1, 2)$ is a generic function, z is the wall-normal distance, $\langle \cdot \rangle$ is the ensemble average of the bracketed quantity, and q_0 is a fixed real number.

According to Townsend's attached-eddy hypothesis, high-Reynolds-number wall-bounded flows may be modeled as collections of wall-attached eddies [14,15]. A primitive flow quantity, e.g., velocity, in the logarithmic region can be computed by adding up incremental contributions from all wall-attached eddies, which may be modeled as random addends, i.e., a_i and b_i [18,21],

$$u = \sum_{i=1}^{N_z} a_i, \qquad v = \sum_{i=1}^{N_z} b_i, \tag{1}$$

where the number of addends is

$$N_z = \int_z^\delta \rho(z) dz \sim \ln(\delta/z). \tag{2}$$

A self-repeating process similar to the one in Eq. (1) was previously used to generate fractals and intermittent turbulent dissipation signals [22,23], and depending on the statistical properties of a_i and b_i, the resulting streamwise and spanwise velocity signals can have very different statistical properties. Here $\rho(z)$ is the eddy population density, and because the eddies are wall attached and space filling, $\rho(z)$ scales as $\sim 1/z$ and δ is the boundary layer height. Since the attached eddies are

TABLE I. Details of the hot-wire measurements. Here T is the time of the measurement, dt is the temporal resolution, the superscript $+$ indicates normalization by wall units, and U_∞ is the freestream velocity.

Re_τ	TU_∞/δ	dt^+	U_∞ (m/s)	u_τ (m/s)
2700	2.13×10^4	0.542	20.0	0.733
4200	1.79×10^4	0.508	20.0	0.710
5800	1.56×10^4	0.476	22.0	0.687
7800	1.38×10^4	0.466	20.1	0.683
10 000	1.59×10^4	0.444	20.0	0.659
13 000	1.16×10^4	0.410	20.0	0.639

self-similar and noninteracting, both a_i and b_i are independent and identically distributed random addends. The last modeling assumption conveniently lends u and v to the large-deviation theory (LDT). According to the LDT [24], for a reasonably large N_z, the far tail of the streamwise velocity PDF $P(u)$ is

$$P(u/N_z) \sim \exp[-N_z f(u/N_z)], \tag{3}$$

where the function f is

$$f = \mathcal{L}[\tau(q)], \tag{4}$$

with

$$\tau(q) = \ln[\langle \exp(qa) \rangle] = \ln[\langle \exp(qu) \rangle]/N_z. \tag{5}$$

Here $\mathcal{L}[\cdot]$ is the Legendre transformation of the bracketed function.

The number of addends, i.e., the scaling factor N_z, is $\sim \ln(\delta/z)$ [Eq. (2)], but it could also be a statistic that follows a $\ln(\delta/z)$ scaling. It follows from Eq. (1) that both

$$\langle u^2 \rangle = \left\langle \left(\sum_{i=1}^{N_z} a_i \right)^2 \right\rangle = N_z \langle a^2 \rangle + \sum_{i \neq j} \langle a_i a_j \rangle = N_z \langle a^2 \rangle \sim \ln(\delta/z) \tag{6}$$

and

$$\ln\langle \exp(q_0 u) \rangle = \ln[\langle \exp(q_0 a) \rangle^{N_z}] \sim \ln(\delta/z) \tag{7}$$

are viable scale factors. Here $\langle a_i a_j \rangle = 0$ $(i \neq j)$ because the addends are statistically independent and $\langle a_i^2 \rangle = \langle a_j^2 \rangle$ because the addends are statistically identical. Hence

$$N_z \sim \ln(\delta/z) \sim \langle u^2 \rangle \sim \ln[\langle \exp(q_0 u) \rangle]. \tag{8}$$

Because the boundary layer thickness is not locally defined, i.e., one would have to measure the whole boundary layer to determine the boundary layer height, depending on the data availability, it may be more convenient to use a locally defined scale factor like $\langle u^2 \rangle$ or the moment generating function. Conclusions of the LDT are formally valid only when N is very large. A brief discussion of how large N has to be may be found in, e.g., [23], and $N = \log_2(2^{12})$ is usually a good number. For a $\mathrm{Re}_\tau = 10\,000$ boundary layer, the number $N = \log_2(10\,000) \approx \log_2(2^{13})$, which is not bad. The number N is certainly not large at moderate Reynolds numbers, but we will show that our model works reasonably well at $\mathrm{Re}_\tau \approx 1000$.

To briefly summarize, the scaled velocity PDF

$$\ln[P(u/N_z)]/N_z$$

TABLE II. Details of the cross-wire measurements. The streamwise and the spanwise velocity fluctuations are measured.

Re_τ	TU_∞/δ	dt^+	U_∞ (m/s)	u_τ (m/s)
10 000	3.8×10^4	0.377	14.79	0.484

is universal. The above equation summarizes the main conclusion of this work. The proposed universality is that the velocity PDFs, if scaled as $\ln[P(u/N_z)]/N_z$, do not depend on the Reynolds number or the wall-normal distance. The spanwise counterparts of Eqs. (3)–(8) can be obtained by replacing u with v in Eq. (3) and a with b in Eq. (5). It is worth noting that, depending on the flow quantity, the predicted asymptotic scaling may emerge at different Reynolds numbers.

Equation (3) is a direct result of the attached-eddy hypothesis. Hence the validity of the model depends on the validity of Townsend's attached-eddy hypothesis. The hypothesis is generally supported by data [16], but one inadequacy of the hypothesis is that it assumes eddies are noninteracting. Recent evidence shows that eddies in boundary layers can interact [25,26] and that may limit the applicability of our model.

III. DATA SETS

To verify the above velocity PDF scaling, we will use both hot-wire measurements and DNS data. The details of the data sets are summarized in Tables I–III. The hot-wire measurements were taken from the High Reynolds Number Boundary Layer Wind Tunnel (HRNBLWT) [8,10] and cover a range of Reynolds numbers from $\mathrm{Re}_\tau \approx 2800$ to $\mathrm{Re}_\tau \approx 13\,000$. The DNS is a channel flow at $\mathrm{Re}_\tau \approx 1000$ [11]. Four thousand snapshots of time-resolved velocity and pressure in the entire channel are publicly available at the Johns Hopkins Turbulence Database (JHTDB).

The convergence of a probability distribution is usually limited by the amount of data and therefore the data at JHTDB and the hot-wire measurements from the HRNBLWT are particularly useful. A few snapshots of channel flow DNS at higher Reynolds numbers are available [12,27], but because of the limited data size, these data will not be very useful here. Unless otherwise noted, all quantities are normalized using wall units, i.e., friction velocity $u_\tau = \sqrt{\tau_w/\rho}$ and viscous length scale ν/u_τ, where τ_w is the mean wall-shear stress and ρ is the fluid density.

At high Reynolds numbers, because of amplitude modulation [28], the flow is only self-similar above $z^+ \approx 3\sqrt{\mathrm{Re}_\tau}$ and therefore we examine Eq. (3) above $z^+ \approx 3\sqrt{\mathrm{Re}_\tau}$. At moderate Reynolds numbers, however, amplitude modulation is not prominent [29] and we expect Eq. (3) to work beyond the logarithmic range.

IV. RESULTS

In Fig. 1(a) we have already shown the streamwise velocity PDF in the logarithmic layer $3\sqrt{\mathrm{Re}_\tau} < z^+, z < 0.2\delta$ [7] for hot-wire measurements of boundary layers at $\mathrm{Re}_\tau \approx 2800$–$13\,000$. The data are not Gaussian [30,31]. Since velocity signals are more intermittent near the wall than

TABLE III. Details of the DNS channel. The two numbers in parentheses are the wall-normal grid spacing at the wall and at the channel center. The superscript + indicates normalization by the wall units, i.e., u_τ and ν/u_τ.

Re_τ	$L_x \times L_y \times L_z$ (δ)	$\Delta x^+ \times \Delta z^+ \times \Delta y^+$
1000	$8\pi \times 2 \times 3\pi$	$12.3 \times (0.0165, 6.16) \times 6.13$

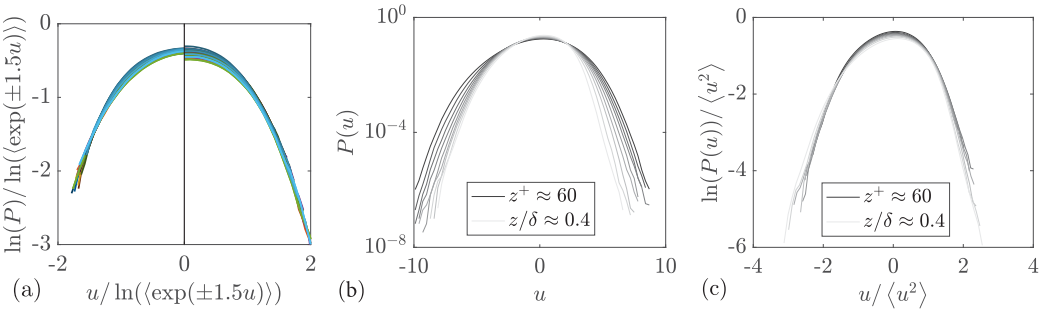

FIG. 2. (a) Scaled streamwise velocity PDF [the scale factor $N_z \sim \ln\langle\exp(\pm q_0 u)\rangle$, where $u < 0$ corresponds to $q_0 = -1.5$ and $u > 0$ corresponds to $q_0 = 1.5$]. (b) Logarithm of the unscaled streamwise velocity PDF at wall-normal distances from $z^+ \approx 60$ to $z/\delta \approx 0.4$ in a DNS channel flow at $\mathrm{Re}_\tau = 1000$. Darker colors are for data closer to the wall. The wall-normal distances are logarithmically spaced from $z^+ \approx 60$, and $z/\delta \approx 0.4$. (c) Logarithm of scaled velocity PDF $P/\langle u^2\rangle$.

they are away from the wall, no data collapse can possibly be found. Figure 2(a) shows the scaled velocity PDF. The data collapse. The wiggles at the tips are probably due to a lack of statistical convergence. The scale factor N_z is $\ln[\langle\exp(\mp q_0 u)\rangle]$ for $u \lessgtr 0$, respectively. The moment generating function $\langle\exp(q_0 u)\rangle$ emphasizes velocity fluctuations that have the same sign as q_0. Considering the asymmetry of the streamwise velocity PDF, we have used positive q_0 to scale the positive side of the velocity PDF and vice versa. The value $q_0 = 1.5$ is arbitrary, and using $q_0 = 1.0, 2.0$ leads to very similar results (see Fig. 3). The scaled velocity PDF is discontinuous at $u = 0$ because q_0 abruptly changes value from -1.5 to 1.5 across $u = 0$. Figures 2(b) and 2(c) show the unscaled and scaled streamwise velocity PDF at wall-normal distances from $z^+ \approx 60$ to $z/\delta \approx 0.4$ in a $\mathrm{Re}_\tau \approx 1000$ channel. The scale factor is $N_z \sim \langle u^2\rangle$. The same observation as for Figs. 1(a) and 2(a) can be made. The theory promises that the scaled velocity PDFs collapse as long as they are scaled using one of the scale factors in Eq. (8). The fact that the velocity PDFs collapse for different scale factors shows the strong predictive power of our theory.

The same exercise can be done for the spanwise velocity and using the scale factors $N_z \sim \ln(\delta/z)$. Figures 4(a)–4(d) show the scaled and unscaled spanwise velocity PDFs at $\mathrm{Re}_\tau \approx 10\,000$ (hot-wire boundary layer) and $\mathrm{Re}_\tau = 1000$ (DNS channel), respectively. The scale factors are $N_z \sim \ln[\langle\exp(v)\rangle]$ and $\ln(\delta/z)$, respectively. Cross-wire measurements of the spanwise velocity component are not available at other Reynolds numbers. For the spanwise velocity, $\langle\exp(-v)\rangle = \langle\exp(v)\rangle$ and therefore we have used $N_z \sim \ln[\langle\exp(v)\rangle]$ to scale both v and $-v$. Both scale factors are able to collapse the data.

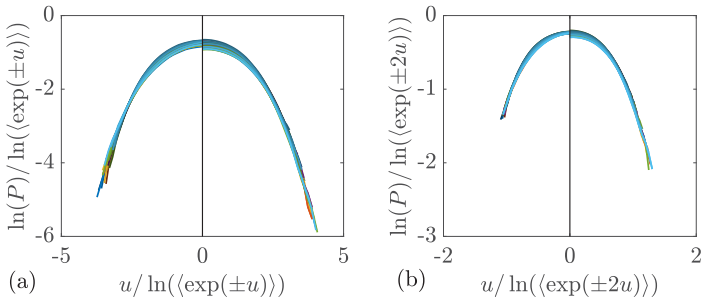

FIG. 3. (a) Same as Fig. 2(a) but using a different $q_0 = 1$. (b) Same as Fig. 2(a) but using a different $q_0 = 2$.

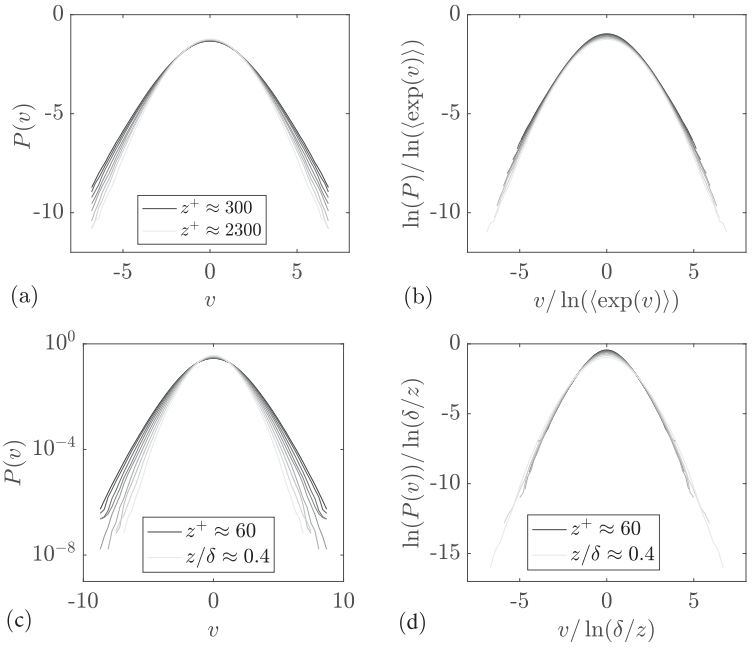

FIG. 4. (a) Spanwise velocity PDF within $3\sqrt{\mathrm{Re}_\tau} < z^+, z < 0.2\delta$. Data at $\mathrm{Re}_\tau \approx 10\,000$ are shown. Darker colors are used for data closer to the wall. (b) Scaled spanwise velocity PDF [the scale factor $N_z \sim \ln\langle\exp(v)\rangle$]. (c) Unscaled spanwise velocity PDF in a channel at $\mathrm{Re}_\tau \approx 1000$. The legends are the same as in Fig. 2(c). (d) Same as (c) but for the scaled velocity PDF.

The above analysis confirms the proposed universality, lending support to the Townsend attached-eddy hypothesis, which models the velocity fluctuations as results of self-repeating processes. Next we compare the scaled PDF to $f = \mathcal{L}[\tau(q)]$. The spanwise velocity is more intermittent than its streamwise counterpart and therefore presents a more challenging case. Figure 5(a) shows the measured exponent $\tau(q)$. The spanwise moment generating function $\langle\exp(qv)\rangle$ is a power-law function of the wall-normal distance and $\tau(q)$ is the corresponding power-law exponent, which can be directly measured following Refs. [21,32]. We compare $-c' + f$ to $\ln(P)/c\ln(\delta/z)$ in Fig. 5(b), where c and c' are constants [note that Eqs. (4) and (8) give only the scaling and there are undetermined constants]. The data are seen to follow f closely. The above exercise may be done for the streamwise velocity and the results are very similar (not shown). It is worth noting that Eq. (4)

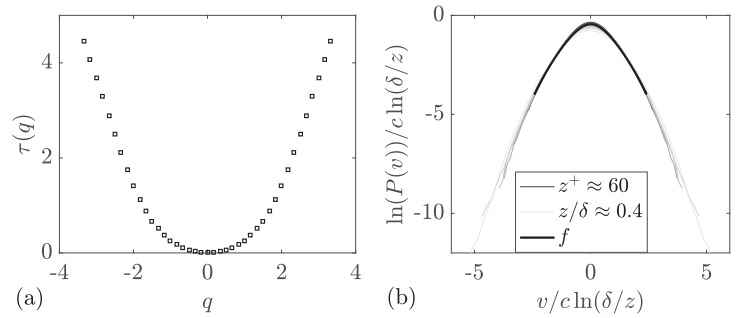

FIG. 5. (a) Measured $\tau(q)$ as a function of q. (b) Plot of $\ln(P)/c\ln(\delta/z)$ and $c' - f_1$. The two constants are $c = 1.26$ and $c' = 0.45$.

is only useful if the knowledge of the function behavior of the single-point moment generating function is available.

V. CONCLUDING REMARKS

In conclusion, the velocity PDF tails collapse if scaled according to Eqs. (3) and (8). Because Eq. (3) is a direct consequence of the attached-eddy hypothesis and the LDT, the work lends strong support to the attached-eddy hypothesis and therefore Eq. (1). While not formally shown here, the theory holds as long as the quantity in question results from a self-repeating process and can therefore be leveraged to predict the sizes of rocks and the lengths of twigs, both of which are results of self-repeating processes.

ACKNOWLEDGMENTS

We gratefully acknowledge C. Meneveau and P. Johnson for fruitful discussion. M.-W.G. would like to thank the China Scholarship Council to support his visit to Penn State. This work was financially supported by Penn State University, Australian Research Council, and the National Natural Science Foundation of China (Grant No. 11772128).

[1] A. J. Smits, B. J. McKeon, and I. Marusic, High-Reynolds number wall turbulence, Annu. Rev. Fluid Mech. **43**, 353 (2011).
[2] S. B. Pope, PDF methods for turbulent reactive flows, Prog. Energy Combust. Sci. **11**, 119 (1985).
[3] D. C. Haworth, Progress in probability density function methods for turbulent reacting flows, Prog. Energy Combust. Sci. **36**, 168 (2010).
[4] P. S. Klebanoff, Characteristics of turbulence in boundary layer with zero pressure gradient, Tech. Rep. NACA-TR-1247, 1955.
[5] S. P. G. Dinavahi, K. S. Breuer, and L. Sirovich, Universality of probability density functions in turbulent channel flow, Phys. Fluids **7**, 1122 (1995).
[6] B. Lindgren, A. V. Johansson, and Y. Tsuji, Universality of probability density distributions in the overlap region in high Reynolds number turbulent boundary layers, Phys. Fluids **16**, 2587 (2004).
[7] I. Marusic, J. P. Monty, M. Hultmark, and A. J. Smits, On the logarithmic region in wall turbulence, J. Fluid Mech. **716**, R3 (2013).
[8] N. Hutchins, T. B. Nickels, I. Marusic, and M. S. Chong, Hot-wire spatial resolution issues in wall-bounded turbulence, J. Fluid Mech. **635**, 103 (2009).
[9] M. Hultmark, M. Vallikivi, S. C. C. Bailey, and A. J. Smits, Turbulent Pipe Flow at Extreme Reynolds Numbers, Phys. Rev. Lett. **108**, 094501 (2012).
[10] K. M. Talluru, R. Baidya, N. Hutchins, and I. Marusic, Amplitude modulation of all three velocity components in turbulent boundary layers, J. Fluid Mech. **746**, R1 (2014).
[11] J. Graham, K. Kanov, X. I. A. Yang, M. Lee, N. Malaya, C. C. Lalescu, R. Burns, G. Eyink, A. Szalay, R. D. Moser, and C. Meneveau, A Web services accessible database of turbulent channel flow and its use for testing a new integral wall model for LES, J. Turbul. **17**, 181 (2016).
[12] M. Lee and R. D. Moser, Direct numerical simulation of turbulent channel flow up to $\mathrm{Re}_\tau \approx 5200$, J. Fluid Mech. **774**, 395 (2015).
[13] Y. Yamamoto and Y. Tsuji, Numerical evidence of logarithmic regions in channel flow at $\mathrm{Re}_\tau = 8000$, Phys. Rev. Fluids **3**, 012602 (2018).
[14] A. A. Townsend, *The Structure of Turbulent Shear Flow* (Cambridge University Press, Cambridge, 1976).
[15] J. D. Woodcock and I. Marusic, The statistical behavior of attached eddies, Phys. Fluids **27**, 015104 (2015).
[16] I. Marusic and J. P. Monty, Attached eddy model of wall turbulence, Annu. Rev. Fluid Mech. **51**, 49 (2019).

[17] X. I. A. Yang, I. Marusic, and C. Meneveau, Hierarchical random additive process and logarithmic scaling of generalized high order, two-point correlations in turbulent boundary layer flow, Phys. Rev. Fluids **1**, 024402 (2016).

[18] X. I. A. Yang and C. Meneveau, Hierarchical random additive model for wall-bounded flows at high Reynolds numbers, Fluid Dyn. Res. **51**, 011405 (2018).

[19] X. I. A. Yang and A. Lozano-Durán, A multifractal model for the momentum transfer process in wall-bounded flows, J. Fluid Mech. **824**, R2 (2017).

[20] X. I. A. Yang, R. Baidya, P. Johnson, I. Marusic, and C. Meneveau, Structure function tensor scaling in the logarithmic region derived from the attached eddy model of wall-bounded turbulent flows, Phys. Rev. Fluids **2**, 064602 (2017).

[21] X. I. A. Yang, C. Meneveau, I. Marusic, and L. Biferale, Extended self-similarity in moment-generating-functions in wall-bounded turbulence at high Reynolds number, Phys. Rev. Fluids **1**, 044405 (2016).

[22] P. Polotti and G. Evangelista, Fractal additive synthesis via harmonic-band wavelets, Comput. Music J. **25**, 22 (2001).

[23] C. Meneveau and K. R. Sreenivasan, Simple Multifractal Cascade Model for Fully Developed Turbulence, Phys. Rev. Lett. **59**, 1424 (1987).

[24] A. Shwartz and A. Weiss, *Large Deviations for Performance Analysis: Queues, Communication and Computing* (CRC, Boca Raton, 1995), Vol. 5.

[25] I. Marusic, R. Mathis, and N. Hutchins, Predictive model for wall-bounded turbulent flow, Science **329**, 193 (2010).

[26] M. F. Howland and X. Yang, Dependence of small-scale energetics on large scales in turbulent flows, J. Fluid Mech. **852**, 641 (2018).

[27] A. Lozano-Durán and J. Jiménez, Effect of the computational domain on direct simulations of turbulent channels up to $\mathrm{Re}_\tau = 4200$, Phys. Fluids **26**, 011702 (2014).

[28] R. Mathis, N. Hutchins, and I. Marusic, Large-scale amplitude modulation of the small-scale structures in turbulent boundary layers, J. Fluid Mech. **628**, 311 (2009).

[29] X. I. A. Yang and M. F. Howland, Implication of Taylor's hypothesis on measuring flow modulation, J. Fluid Mech. **836**, 222 (2018).

[30] F. Durst, J. Jovanovic, and L. Kanevce, in *Turbulent Shear Flows 5*, edited by F. Durst, B. E. Launder, J. L. Lumley, F. W. Schmidt, and J. H. Whitelaw (Springer, Berlin, 1987), pp. 197–220.

[31] F. N. Frenkiel and P. S. Klebanoff, Probability distributions and correlations in a turbulent boundary layer, Phys. Fluids **16**, 725 (1973).

[32] X. I. A. Yang, I. Marusic, and C. Meneveau, Moment generating functions and scaling laws in the inertial layer of turbulent wall-bounded flows, J. Fluid Mech. **791**, R2 (2016).